

FINITE ELEMENT MODELLING OF STONE COLUMN INSTALLATION: REVIEW OF MODELLING PRACTICES AND CASE STUDY WITH PLAXIS 2D



*Challenges from North to South
Des défis du Nord au Sud*

Olivier Hurley, Mathieu Nuth, Mourad Karray

Department of Civil engineering – Université de Sherbrooke, Sherbrooke, Quebec, Canada

ABSTRACT

This article discusses the different numerical modelling practices for the stone column installation and establishes a comparative review of the numerical techniques and constitutive laws used in the literature. Furthermore, taking advantage of the best practices in numerical modelling of stone column installation, a numerical model was created with PLAXIS 2D in axisymmetric geometry to reproduce the lateral expansion of stone in sand. The host material is modelled with a hardening soil constitutive relation to represent the repetitive loading and unloading of the sand during expansion. The results are presented in terms of lateral to vertical stress ratio and variation in void ratio and are then calibrated with two experimental stone column tests carried out at an intermediate scale in our laboratory.

RÉSUMÉ

Cet article présente une étude comparative des différentes techniques de modélisation numérique de la mise en place des colonnes ballastées ainsi que les lois constitutives utilisées dans la littérature pour bien représenter les mécanismes rencontrés. Par la suite, prenant en compte la bonne pratique en modélisation numérique, une analyse 2D axisymétrique est réalisée avec PLAXIS 2D comprenant l'utilisation d'une loi d'écrouissage isotrope (Hardening Soil Model) pour le sol encaissant qui est un sable fin. Cette loi d'écrouissage permet de bien représenter le chargement répétitif du sable causé par l'expansion graduelle de la colonne de pierre dans le sol. Cette analyse numérique est vérifiée par comparaison avec les résultats de deux colonnes ballastées de grandeurs intermédiaires réalisés en laboratoire par rapport au coefficient de pression des terres après la mise en place et la variation de l'indice des vides.

1 INTRODUCTION

The construction of stone columns is a common practice for soil improvement. The improvement addresses an insufficient bearing capacity (granular or cohesive materials), an excessive settlement (total or differential) or a liquefaction potential. The most common method is the well-known vibro-replacement technique which can be applied with or without water or air injection.

This technique uses a long vibrating probe with either stone insertion from the top (top feed) with a loader or from the bottom (bottom feed) of the hole. It creates a column from the repetitive up and down motion of the probe and continuous feeding of the stone. A meshing of columns is then created at a certain radius to generalise the improvement to the desired in an area.

Despite the fact that the soil improvement is efficient and can be measured on site with standard testing, the mechanics involved in the improved characteristics still need to be understood and modeled. This research paper discusses the main design methods for stone column using vibro-replacement method and its application in numerical modelling practices. Furthermore, a numerical analysis was performed to recreate the stress field and the modified void ratio after the installation a stone column based on the experiment by Hurley & al. (2013).

2 DESIGN METHODS

A vast number of design methods have been developed to select the right spacing and diameter of stone columns for soil improvement. Many of these design methods rely on the prediction of soil improvement after the installation of stone columns. The in-situ, lateral stress on the stone column is believed to have a major impact on their behavior, since it pilots the confinement stress resisting against shear.

Another parameter that reflects the improvement of the native soil is the increase in relative density, characterized as the increase of void ratio. There are two aspects to this parameter, the initial void ratio and the final void ratio which are usually both estimated or correlated from field tests.

In an infinitely large soil layer, the increase in lateral stress and in relative density will fade over a certain distance from the column until the initial in situ soil state is reached. The main purpose of the design methods is overlapping the effective improved areas between each column to reach a global soil improvement that fits the design needs, i.e.: proper bearing capacity, limiting settlement, mitigating soil liquefaction or consolidating clay.

Some design methods are empirically based (Mattes & Poulos, 1969), others analytical with linear elasticity (Bouassida & al. 2003; Balaam and Booker 1981) or elastoplasticity (Priebe and Grundbau 1995; Ghionna and Jamiolkowski, 1981; Goughnour and Bayuk, 1979). Usually, these methods are used in order to define the replacement ratio, or in other words the stone column

diameter and spacing geometry, which will provide the maximum bearing capacity or the maximum settlement of a reinforce soil.

Most design methods use a triangular or rectangular mesh and the unit cell concept as explain in Figure 1, where \varnothing_e is the effective diameter, \varnothing_{sc} is the stone column diameter, s the spacing, q_0 the surcharge and SC the stone column itself.

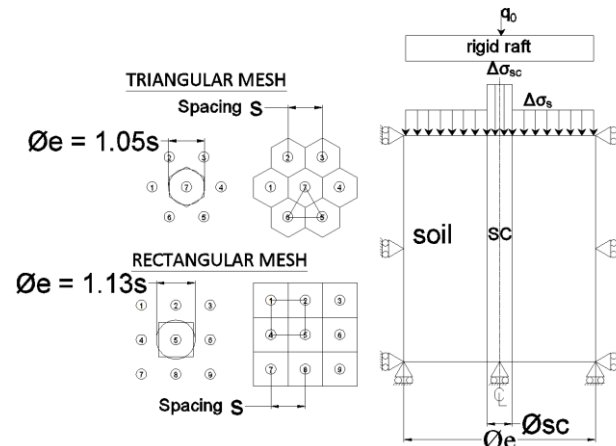


Figure 1: Design meshes (left) and unit cell concept (right) – adapted from Goughnour and Bayuk, 1979

Seed & Booker (1976) are the first researchers to introduce an analytical method based on the radial dissipation of pore water pressure during earthquake for soil liquefaction mitigation. Their work led to a well-known design method for stone columns against soil liquefaction by Baez & Martin, (1995) which is still the main reference used in practice to mitigate soil liquefaction using stone columns. However, no detailed description of the lateral to vertical stress ratio is offered in these design methods.

3 NUMERICAL MODELLING OF THE EFFECT OF STONE COLUMN INSTALLATION ON WEAK SOIL

3.1 Main concept

The main concept of the stone column numerical modelling is based on the method of installation and its effect on the soil surrounding the column. To rightfully model the column installation, each step of the column construction needs to be represented by the numerical procedure. For example, the vibro-replacement method consists of the following steps: (1) insertion of the vibrating probe down to the required depth, (2) stone pushing through the end of the probe that is lifted up and down (0,5 m) to compact the stone and expand the diameter until the required length is obtained and (3) repeating the process until the full column is built.

The numerical modelling tries to recreate accordingly the construction processes with certain simplifications. In terms of soil behavior, these processes can be seen as follows: (1) Cavity expansion of the soil, from a nil radius to a radius equal to the probe diameter (Vesic 1972); (2) Gradual lateral loading of the surrounding soil caused by the insertion of stone and the expansion of the stone

column into the soil; (3) creating a group effect of columns representing the meshing geometry.

3.2 State of the art

The effect of stone column installation on the surrounding soil is quite recent. The numerical modeling of stone column installation started around 2001. Numerous numerical procedures were developed to model the stone column installation. Some authors impose a uniform lateral displacement equal to the final stone column average diameter using a axisymmetric model in 2D (Guétif and al. 2007; Castro and Karstunen 2010; Kirsch 2006), others use a uniform volumetric strain expansion of the stone column in 3D (Foray and al., 2009) and some authors performed a back analysis by varying the lateral to vertical stress ratio (K) to obtain the field test behavior (Elshazly and al. 2008; Elshazly and Hafez 2006).

Most of the numerical methods were performed and calibrated for clays, where the effect of the vibrating probe would be nil as in the case of the vibro-replacement technique. The main effect in clay would be caused by a lateral expansion of the stone column in an undrained weak soil. This would lead to an increase of pore water pressure and an increase of lateral to vertical stress ratio (K) on the stone column. In this case, the soil density increases from the consolidation of the clay and the stress ratio is increased with the density of the mesh of columns (group effect). It has been demonstrated by Foray and al. (2009) that to better account for the group-effect on the surrounding soil, it is more appropriate to model in 3D rather than in 2D. Egan and al. (2009) also suggest using a volumetric strain expansion of the stone columns rather than an imposed lateral displacement

Little study has been made to consider the interaction between the vibrating needle, the expansion of the cavity and the increased of lateral to vertical stress ratio in sand. Having a much higher permeability coefficient than clay and no cohesion, sand will liquefy during installation. This will lead to a densification of the soil also amplified by the expansion of the stone column until the final diameter is reached. Shenthan and al. (2006) propose a coupled model where mechanical expansion and dynamic vibration is coupled with an increase in pore water pressure. Their studies have led to the use of wick drains in the center of a mesh when the fine content is higher than 15%. This leads to a better dissipation of water pressure during construction and consequently of an increase in relative density.

The modelling of vibration in dry sand has been investigated firstly by Kessler and al. 2006 and afterwards by Arnold and al. (2009) using ABAQUS both in 3D and 2D. They represented the vibrating probe as a source generating a cyclic loading laterally on the soil. Although the soil liquefaction during installation was not taken into consideration, they discovered that for this type of modeling, to evaluate the effect of densification on the sand, a 2D axisymmetric model is enough. Also, the boundary condition can have considerable effect on the soil behavior during modeling.

3.3 Constitutive laws for soils

Different constitutive laws may be used depending on the part of the stone column and surrounding soil that is modeled. In the context of the numerical modeling of stone column installation, it is more appropriate to use an elastoplastic model such as the Modified Cam-Clay (Schofield and Worth 1968) or the Hardening Soil Model (Schanz et al. 1999) in the case of the surrounding soil (granular or cohesive) to fully represent loading and unloading behavior. This will allow the user to follow the change in density and resistance as the column is constructed. Also, the zones of native soil prone to plasticity, i.e. more permanent deformations and failure, can be identified in the vicinity of the stone column. The process of installation is considered under undrained conditions as the soil does not have time to dissipate the increased pore water pressure. Since in most numerical procedure the stone is not fully modelled during expansion as it can create strong divergence and unnecessary numerical complexity, the stone column is usually modelled as a linear elastic behavior.

If the goal of the model is to study the bearing capacity or settlement characteristic of the new soil-column complex, the soil and stone could be modelled as an elastoplastic model since under long-term, the column will plastify (Castro and Segaseta 2011).

4 NUMERICAL ANALYSIS USING PLAXIS 2D

The main goal of this numerical experiment is to be able to better understand the mechanics involved in the process of stone insertion in a granular medium by comparing experimental results with 2D axisymmetric numerical analysis. The 2D axisymmetric approach is considered as valid for the present study since no group effect needs to be accounted for.

4.1 Laboratory experiment of stone column installation

A laboratory testing experiment was conducted by Hurley & al. (2013) at the Université de Sherbrooke. The goal was to measure the increase of lateral to vertical stress ratio and the variation of relative density during and after stone insertion. A unique apparatus was constructed to apply and monitor a vertical stress on a clean sand sample to represent different depth. The lateral stress was monitored in the center of the PVC cell using a paper thin flexible sensor made by Tekscan®. With this sensor it was possible to increase accuracy by averaging the lateral stress on a wide surface instead of usual single load cell.

The apparatus was constructed to allow the insertion of stone in its center while maintaining the vertical stress on the sample. Figure 2 shows the apparatus and the main aspects.

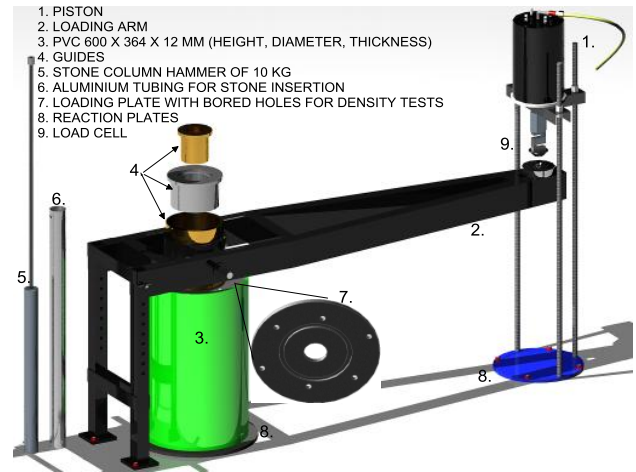


Figure 2: 3D drawing of the physical model apparatus for stone column installation

During this experimental phase, 3 stone columns were created. For the purpose of this article only two columns were used for comparison with the numerical model.

The following parameters for each stone column (SC) are presented in Table 1: average vertical stress (q_0) and its corresponding standard defiation, the average stone column diameter ($\bar{\phi}_{SC}$), the initial relative density (Dr_0), the final relative density (Dr_f) and the dry unit weight of the stone column ($\gamma_{d,SC}$) were calculated using the average stone column diameter, the replacement ratios (Ar), the sand's initial water content ($w_{s,0}$), the initial coefficient of earth pressure at rest (K_0) and the final lateral to vertical pressure ratio (K_f).

Table 1: Stone column construction information

Parameters	SC #1	SC #2
$q_0 \pm \sigma$ (kPa)	101.5 \pm 0.8	81.7 \pm 0.7
$\bar{\phi}_{SC}$ (mm)	74.5	73.5
Dr_0 (%)	45.9	46.2
Dr_f (%)	54.6	54.2
$\gamma_{d,SC}$	18.3	16.2
Ar (%)	4.2	4.1
$w_{s,0}$ (%)	9.0	10.0
K_0	0.31	0.32
K_f	1.32	1.32
$\sigma_{h,res}$	-	-

During the experimental phase, stone was inserted and compacted in the cavity at the center of the cell and by doing so, the stone would push the sand laterally. The vertical stress was maintained constant on the surrounding soil, so the final stress ratio shows the increase in lateral stress caused by the insertion of stone. The stone column was constructed by layers. Each layer was compacted until refusal using a 10 kg hammer. The final diameter was measured after the tests and averaged. Knowing the amount of stone, it was possible to estimate the final relative density of the sand. In order to double

check the results, another test was performed to evaluate the final relative density, a Dynamic Penetration Test which consist of a steel rod with a conic end. It was conducted at three (3) different radius from the center of the cell. The results were then compared to reference curves for improvement estimation.

4.2 Numerical model geometry and analysis procedure

The goal of the numerical analysis using PLAXIS 2D 2012 is to reach the same final lateral stress ratio and the final relative density as for the experiment.

To achieve this goal, the unit cell model was recreated using an axisymmetric geometry where the center of revolution was the center of the cell. After the stress initialization with the k_0 procedure, the sand was loaded with a parabolic vertical stress of 100 kPa in stone column #1 and 80 kPa for stone column #2, representing a depth of approximately 5 and 4 m respectively. The parabolic distribution was preferred over a uniform distribution to better represent the applied load tested in the laboratory.

Castro & Karstunen (2010) reported that a lateral displacement was more numerically stable than a volumetric strain expansion to model the cavity expansion of stone column installation. Although this is true for a uniform displacement along the length of the column like the study by Guétif & al. (2007), it does not allow the modeling of the stone insertion in layers since the deformation between layers is too large and the software cannot converge adequately.

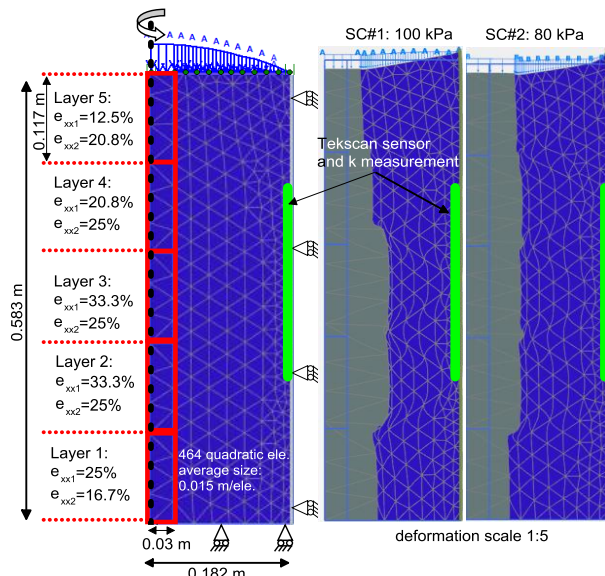


Figure 3: Model geometry and dimensions

A total of five layers were laterally expanded one after the other, with amplitudes of expansion that are conform to the ones measured in the test. After each volumetric strain expansion and before another layer could be expanded, a cavity was created and the material was replaced with the stone material. This allowed the soil to be loaded then unloaded repeatedly (hardened) as the column was being build. Each volumetric strain expansion

corresponded to the average diameter measured during the experimental phase. The updated mesh option was selected to allow large deformations and a change in void ratio. The geometry of the numerical model is presented in detail in Figure 3 with the final shape of both stone columns tested considering a deformed mesh enhanced by a factor of five.

4.3 Soil behavior model

The hardening soil model (HSM) was selected for the analysis of sand. This model was first developed as a mean to overcome the limitation of the Duncan & Chang (1970) hyperbolic model such as loading and unloading behavior and the collapse load computations in the fully plastic range (Schanz & al. 1999). The hardening (plastic straining) is predicted through the expansion of the yield surface in the principal stress space. Isotropic hardening behavior is possible in both shear and compression loadings.

Laboratory testing was performed on the sand to characterise its behavior. A series of 6 direct shear tests combined with modified Proctor tests and oedometer tests allowed for the characterisation of the resistance parameters. The laboratory oedometer tests were fitted with the numerical test as shown on Figure 4 in the calibration module Soiltest from PLAXIS 2D 2012. The stone column was modeled using a linear elastic perfectly plastic model (Mohr-Coulomb - MC) with parameters estimated from literature.

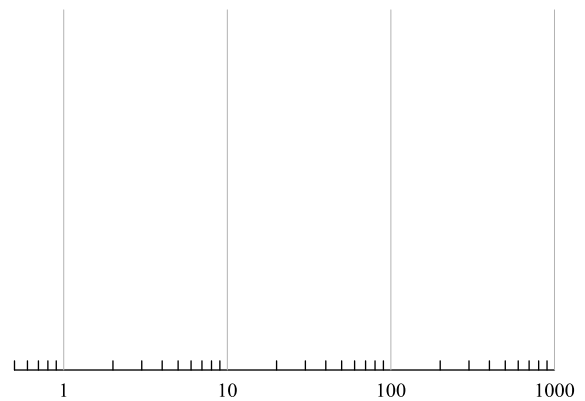


Figure 4: Experimental and numerical oedometer tests

The main parameters for the soil behavior laws are defined in The elastic moduli are defined as follows: E_{50}^{ref} is the elastic modulus at 50% yield and equal to half the unloading-reloading modulus (E_{ur}^{ref}); E_{oed}^{ref} stands for the uniaxial compressive modulus calculated from the compression index (Cc) measured with the oedometer test. The exponent m regulates the non-linearity of the soil elastoplastic behavior and 0.5 is recommended from granular materials. The void ratios are measured during the experimental phase. The interface between the PVC cell and the soil is defined with R_{inter} which is the ratio between the angles of friction of the two material. A value of 0.44 is based on the results of O'Rourke (1990) with

direct shear tests between PVC oil pipes and granular materials.

Table 2 for the sand and the stone. The use of a cohesion for the stone is only to allow the stone column to keep its final shape after the numerical expansion phase. Having a small value of cohesion for the sand helps numerical calculation (PLAXIS 2012). In order to allow the final diameter to be maintained after each layer expansion a cohesion of 10 kPa was used.

The elastic moduli are defined as follows: E_{50}^{ref} is the elastic modulus at 50% yield and equal to half the unloading-reloading modulus (E_{ur}^{ref}); E_{oed}^{ref} stands for the uniaxial compressive modulus calculated from the compression index (Cc) measured with the oedometer test. The exponent m regulates the non-linearity of the soil elastoplastic behavior and 0.5 is recommended from granular materials. The void ratios are measured during the experimental phase. The interface between the PVC cell and the soil is defined with R_{inter} which is the ratio between the angles of friction of the two material. A value of 0.44 is based on the results of O'Rourke (1990) with direct shear tests between PVC oil pipes and granular materials.

Table 2: Parameters for the soil behavior models

SAND (HSM)		STONE (MC)	
Parameters	Values	Parameters	Values
E_{50}^{ref} E_{50}^{ref} (kPa)	16 500	E (kPa)	38 000
E_{oed}^{ref} E_{oed}^{ref} (kPa)	14 700	ν'	0.33
E_{ur}^{ref} E_{ur}^{ref} (kPa)	33 000	c' (kPa)	10
m	0.5	ϕ' (°)	38
ϕ' (°)	35	ψ (°)	8
c'_{ref} (kPa)	0.1	γ (kN/m ³)	20
ψ (°)	5.7		
γ_{sat} (kN/m ³)	18.1		
e_{min}	0.47		
e_{max}	0.75		
R_{inter}	0.44		

During the experimental phase, the sand was placed on the dry side of the optimal water content ($9.6 \pm 0.5\%$). Since it was unsaturated during the experiment, there was no pore water pressure build up calculated during the numerical analysis. The stress is then calculated and expressed as total stresses.

4.4 Results

4.4.1 Effect of installation on lateral to vertical stress ratios

The lateral to vertical stress ratio were calculated in the unit cell model and compared to the values measured during the experiment. The stress ratio was measured at the same location as the Tekscan sensor. The relative density was measured at the same three (3) radius (R) from the center as for the Dynamic Penetration Tests (DPT) during the experiment.

Table 3 summarizes the results from the stress ratio measurement. Figure 5 compares the increase of lateral stress measured on the Tekscan sensor and the one calculated numerically.

Table 3: comparison of experimental measurements and numerical calculation of horizontal and vertical stresses

	SC #	σ_x	σ_y	k	Error (%)
Exp.	1	147	107	1.38	0.16
Num.		146.7	107.0	1.37	
Exp.	2	122	88.6	1.39	0.40
Num.		121.0	87.3	1.39	

Experimentally, it is clear that each compacted layer gradually increases the stress on the sensor. Similarly, each of the five (5) volumetric strain expansion increases the stress measured at the same location. After completion the stress was maintained during a certain time to verify the stability of the physical model. For both stone columns tested, the error measured with regard to the stress ratio at the end the analysis and the experiment is less than 1%.

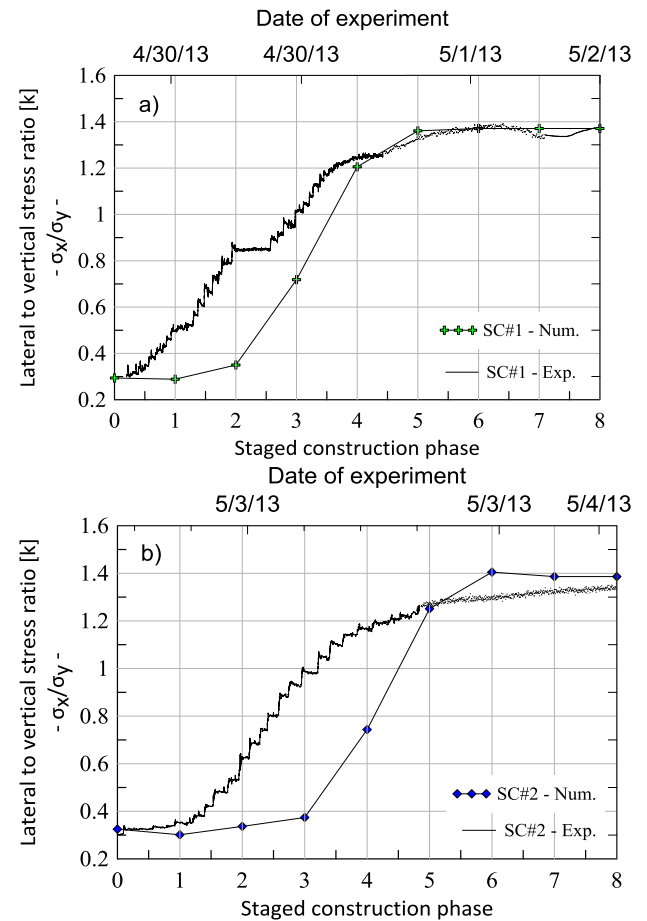


Figure 5: Comparison of lateral to vertical stress ratios after experimental and numerical analysis for a) SC #1 and b) SC #2

4.4.2 Effect of installation on the relative density of the surrounding sand

The relative density was measured with the dynamic penetration tests as explained in detail by Hurley & al. 2013. The location is indicated on the side images to the plots on Figure 6.

The stone column diameter was also measured at different depths during the excavation of the surrounding soil after testing. This allowed for the interpretation of the average relative density of the sand after stone insertion as it can be shown on Figure 6 with the full blue line.

It is clear from the comparison of the numerical data and the experimental data that the numerical analysis predicted very effectively the final relative density of the sand. On average, the relative density calculated numerically was 52.6% and 52.3% for SC #1 and #2 respectively and 54.6% and 54.2% respectively for the experiment.

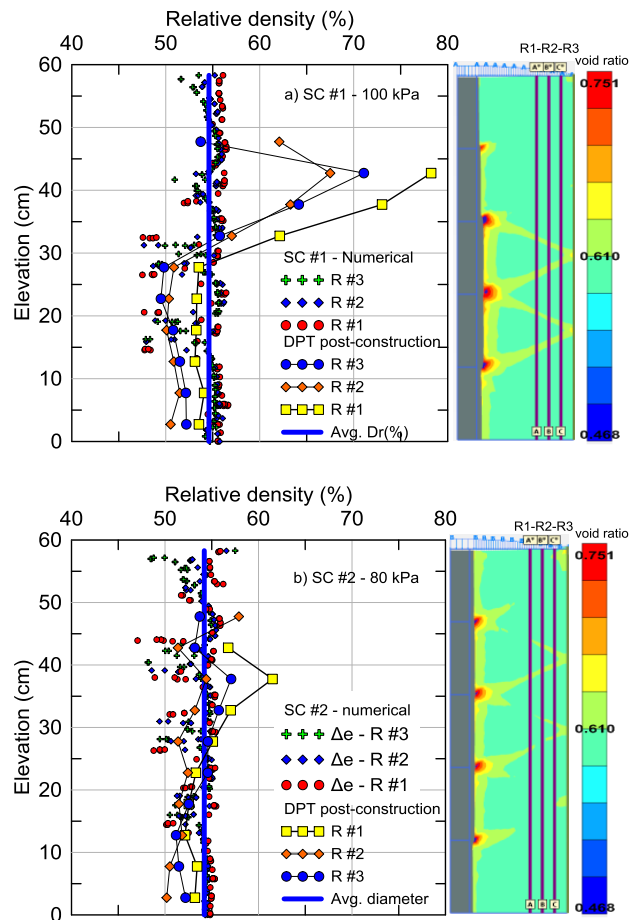


Figure 6: Effect of installation of stone columns on the relative density of the sand – Comparison between experimental data and numerical analysis a) SC #1 b) SC #2. [SC: stone column, R: Radius, DPT: Dynamic penetration test]

Although the main goal of the 3 radius for the DPTs was to measure the variation of the relative density with

distance, the proximity of each test did not show much difference either numerically as experimentally.

Also, it is possible to see the local shear zones between each layer expansion. This is caused because during the volumetric strain expansion, the soil is not equally solicited. During each expansion, the junction between two layers would create a zone of local shear and expansion. This would cause the soil to rupture along the axes shown in yellow on the side images.

5 DISCUSSION & CONCLUSION

The results presented in the last section show a good convergence between the measures values and the calculated values of lateral to vertical stress ratio and finale relative density.

This was obtained by using a volumetric strain expansion of five layers with an updated mesh calculation rather than a more common practice of using a uniform lateral displacement. A final stress ratio ± 1.4 is comparable to other studies as can be shown in Table 4, which provides an interesting insight into the evolution of K during the insertion of a stone column in a scale model.

Table 4: stress ratio comparison with other studies

STUDIES	STRESS RATIO (K)	ENCAISSING SOIL	IN SITU, NUMERICAL OR ANALYTICAL
Priebe & Grundbau, 1995	1.0	Clay	analytical
Watts & al., 2000	$K_0 < k < k_p$	Glacial till	in situ
Pitt & al., 2003	$0.4 < k < 2.2$ Avr. 1.2	Clay	in situ
Elshazly & Hafez, 2006	$1.1 < k < 2.5$ Avr. 1.5	Silty sand and sandy clay	In situ & numerical
Goughnour, 1983	$K_0 < k < 1/K_0$	Clay	analytical
Elshazly & al., 2008	$0.7 < k < 2.0$ Avr. 1.2	Silty sand and sandy clay	in situ

ACKNOWLEDGEMENTS

The authors would like to acknowledge the contribution of Geopac inc. & Mitacs Acceleration for the financial support and also Mohamed Chekired from Institut de Recherche d'Hydro-Québec for the supply of the Tekscan sensors.

REFERENCES

Arnold, M. & al. 2009. Comparison of vibrocompaction methods by numerical simulations. *Proc. 2nd International Workshop on Geotechnics of Soft Soils*, CRC Press, Glasgow, Germany, 3-11.

Baez, J. I. et Martin, G. 1995. Permeability and shear wave velocity of vibro-replacement stone columns. *Dans Proceedings of the Conference of the Geotechnical Engineering Division of the ASCE in*

- Conjunction with the ASCE Convention, October 22 - October 26.* ASCE, San Diego, CA, USA, 66-81.
- Balaam, N. P. and Booker, J. R. (1985). Effect of stone column yield on settlement of rigid foundations in stabilized clay. *International Journal for Numerical and Analytical Methods in Geomechanics*, 9(4): 331-351.
- Bouassida, M. & al. 200. Estimation par une approche variationnelle du tassement d'une fondation sur sol renforcé par colonnes ballastées. *Revue Française de Géotechnique*, (102) 21-22.
- Brinkgreve, R.B.J. 2012. PLAXIS 2D Reference Manual 2012. *Plaxis*, Delft, the Netherlands.
- Castro, J. & Karstunen, M. 2010. Numerical simulations of stone column installation. *Canadian Geotechnical Journal*, 47(10) 1127-1138.
- Duncan, J.M. Chang, C. Y. 1970. Nonlinear analysis of stress and strain in soils. *Journal of the Soil Mechanics and Foundations Division, ASCE*, 96(SM5), 1629-1653.
- Egan, D. 2009. Installation effects of vibro replacement stone columns in soft clay. *Proc. 2nd International Workshop on Geotechnics of Soft Soils*, CRC Press, Glasgow, Germany, 23-29.
- Elshazly, H. & Hafez, D. 2006. Back calculating vibro-installation stresses in stone columns reinforced grounds. *Journal of Ground Improvement*, 10(2) 47-53.
- Elshazly, H. & al. 2008. Effect of inter-column spacing on soil stresses due to vibro-installed stone columns: Interesting findings. *Geotechnical and Geological Engineering*, 26(2): 225-236.
- Foray, P., & al. 2009. 3D numerical modeling of stone columns and application. *Proc. 17th International Conference on Soil Mechanics and Geotechnical Engineering*, 3: 2382-2385.
- Ghionna, V. & Jamiolkowski, M. 1981. Colonne di ghiaia. *X Ciclo di conferenze dedicate ai problemi di meccanica dei terreni e ingegneria delle fondazioni metodi di miglioramento dei terreni*, Torino, 507.
- Goughnour, R.R. & Bayuk, A. A. 1979. Analysis of stone column - soil matrix interaction under vertical load. *Ocean Industry*, 1: 271-277.
- Guétif, Z. and al. 2007. Improved soft clay characteristics due to stone column installation. *Computers and Geotechnics*, 34(2) 104-111.
- Kessler, S. & al. 2006. On prediction of vibrocompaction performance using numerical models. *Symposium International TRANSVIB*, 233-242.
- Kirsch, F. 2006. Vibro stone column installation and its effect on ground improvement. *Proc. Geotechnical Engineering for Urban Environment, 2006 - March 24.* Taylor and Francis, Bochum, Germany, 115-124.
- Hurley, O. & al. 2013. Physical modeling of stone column installation in fine sand and its effect on lateral to vertical stress ratio, *Proc. GeoMontreal 2013*, Montreal.
- Mattes, N. S. and Poulos, H. G. 1969. Settlement of single compressible pile. *American Society of Civil Engineers, Journal of the Soil Mechanics and Foundations Division*, volume 95, p. 189-207.
- O'Rourke, T. 1990. Shear-strength characteristics of sand-polymer interfaces. *Journal of Geotechnical Engineering*, volume 116, p. 451-469.
- Priebe, H. J. & Grundbau, K. (1995). Design of vibro replacement. *Ground Engineering*, 28(10): 31-37.
- Schanz, T. Vermeer, P.A. Bonnier, P.G. 1999. The hardening soil model: formulation and verification, *Beyond 2000 in computational Geotechnics – 10 Years of PLAXIS*, Rotterdam.
- Schofield, A. Worth C.P. 1968. *Critical state soil mechanics*, Mc Graw Hill, London.
- Seed, H.B. & Booker, J. R. 1976. Stabilization of Potentially Liquefiable Sand Deposits Using Gravel Drain Systems. *Journal of Geotechnical Engineering Division*, 103(7) 757-68.
- Shenthan, T. 2006. Liquefaction mitigation in silty soils using stone columns supplemented with wick drains, *PhD Dissertation*, State University of New York at Buffalo.
- Vesic, A.S. 1972. Expansion of cavities in infinite soil mass. *Journal of the Soil Mechanics and Foundations Division*, 98: 265-290.